A 5-stage Active Control Method with Online Secondary Path Modelling Using Decorrelated Control Signal

Somanath Pradhan[*], Xiaojun Qiu

Centre for Audio, Acoustics and Vibration, University of Technology Sydney, NSW 2007

Australia

Abstract

Time-varying primary and secondary paths in active control systems degrade the noise control performance. In this paper, a practical method is proposed for active control systems with online secondary path modelling using the decorrelated control signal. The proposed method consists of 5 stages, i.e., primary path estimation, controller initialization, secondary path estimation, primary and secondary path changing detection, and active control operation, where the speed of the secondary path modelling is improved by incorporating decorrelation filters. The simulation results demonstrate the proposed method is capable of tracking the changes in both primary and secondary paths, remodelling the secondary path, and maintaining the noise reduction performance and stability of the system when both primary and secondary paths change.

Keywords: Active control system, online secondary path modelling, decorrelation filter, convergence speed.

[*]Corresponding author

Email addresses: Somanath.Pradhan@student.uts.edu.au (Somanath Pradhan),
Xiaojun.Qiu@uts.edu.au (Xiaojun Qiu)

1. Introduction

The filtered-x least mean square (FxLMS) algorithm commonly used in active noise control (ANC) requires a model of the secondary path of the system. Offline modelling can be used to estimate the secondary path for ANC applications [1]. However, in certain applications, the secondary path is time varying due to the acoustic surrounding, so online secondary path estimation is needed [2, 3].

White noise can be used to estimate the secondary path online [4]. In this method, the injected white noise is mixed with the residual error signal, thereby affecting the noise reduction performance. A two adaptive filter-based method has been proposed in which the modified FxLMS algorithm is used in adapting the control filter and a new variable step size LMS algorithm is used for adapting the secondary path estimation filter [5]. An optimal variable step size algorithm is proposed for updating both the control and secondary path estimation filters along with a self-tuning power scheduling strategy for the auxiliary noise [6]. A power scheduling algorithm is proposed to increase the convergence speed when sudden changes happen in the secondary path [7]. To make it easy for implementation, a three adaptive filter-based ANC system is reported with a simple power scheduling method and regularized step size for secondary path estimation [8].

The control signal can be used for online secondary path modelling as well but often with a biased estimation [9]. An overall online secondary path modelling is capable of reducing the bias by introducing an extra adaptive filter to model the primary path. The LMS algorithm is used to estimate both the primary and the secondary paths simultaneously, while the control filter is updated with the FxLMS algorithm. The convergence of this algorithm is highly reliant on the control signal characteristics. Unlike the white noise injection method, the estimated secondary path must be copied more frequently to the FxLMS algorithm for smooth operation of active control system, which in turn requires faster and reasonable accurate modelling of the secondary path.

A modified FxLMS algorithm based on offline and online secondary path modelling is proposed to control transformer noise [10]. The secondary path estimated offline is used as the initial value for online modelling, which uses control signal for secondary path estimation. An estimate of the primary path obtained offline is also used to remove the disturbance in modelling the secondary path. However, the system fails if the primary path changes. The change in primary path hinders the convergence of the secondary path estimation and ANC operation.

Several active control algorithms that do not require secondary path estimation have been proposed. A direction selection update algorithm can choose either a positive or a negative direction for adaptive control [11]. To increase the converge speed of the algorithm when the phase angle of the secondary path is close to ±90°, a frequency domain delayless subband architecture has been proposed, where four update directions are used to minimize the error signal [12]. Nevertheless, the architecture possesses high computational complexity as the

weight update is performed in frequency domain. To reduce the implementation complexity, a simplified subband structure is proposed, which is more flexible [13]. However, the convergence of these algorithms is much slower than the conventional FxLMS algorithm.

Though the extended adaptive filtering method is capable of estimating the secondary path using the control signal, the performance is deteriorated as the primary noise characteristics changes. An intelligent ANC system should be able to detect the changes in both primary and secondary paths, and remodel those paths for effective operation. This paper proposes a 5-stage active control method with online secondary path modelling using the decorrelated control signal. The contributions made in this paper are: (1) a new systematic method for active control with online secondary path modelling using the control signal, which includes primary path estimation, controller initialization, secondary path estimation, primary and secondary path changing detection, and active control operation; and (2) increasing the modelling speed of the secondary path with the control signal by using decorrelation filters.

2. Proposed Method

Fig. 1 shows the block diagram of the proposed method, which consists of 5 stages, i.e., primary path estimation, controller initialization, secondary path estimation, primary and secondary path changing detection, and active control operation. In the block diagram, three switches, K_1, K_2 and K_3, are used for choosing the active control operation, the primary path modelling and the secondary path modelling, respectively. Fig. 2 presents the flowchart of the proposed method, where the normal noise reduction, primary path modelling accuracy, and secondary path modelling accuracy are assumed to be T_{r0}, T_{p0}, and T_{s0}, respectively. The toggling of three switches associated with different stages and the corresponding operations of the active control system are briefed sequentially.

The first stage is for the primary path estimation. When the system starts, K_1 and K_3 are turned off, and K_2 is turned on. The cancelling signal $s(n)$ and estimated cancelling signal $\hat{s}(n)$ are absent, $p(n)$ and $\hat{p}(n)$ represent the undesired noise and its estimate. The primary path $P(z)$ between the reference microphone and error microphone is estimated using the NLMS algorithm. The adaptive filter estimating the primary path is updated by

$$\mathbf{p}(n+1) = \mathbf{p}(n) + \mu_p \frac{\varepsilon_p(n)\mathbf{x}_p(n)}{\mathbf{x}_p^T(n)\mathbf{x}_p(n)} \tag{1}$$

where $\mathbf{x}_p(n) = [x(n), x(n-1), \ldots, x(n-L_p+1)]^T$ is the L_p sample reference signal vector, μ_p is the step size, and $\varepsilon_p(n) = \varepsilon(n)$ is the error signal when K_1 and K_3 are turned off.
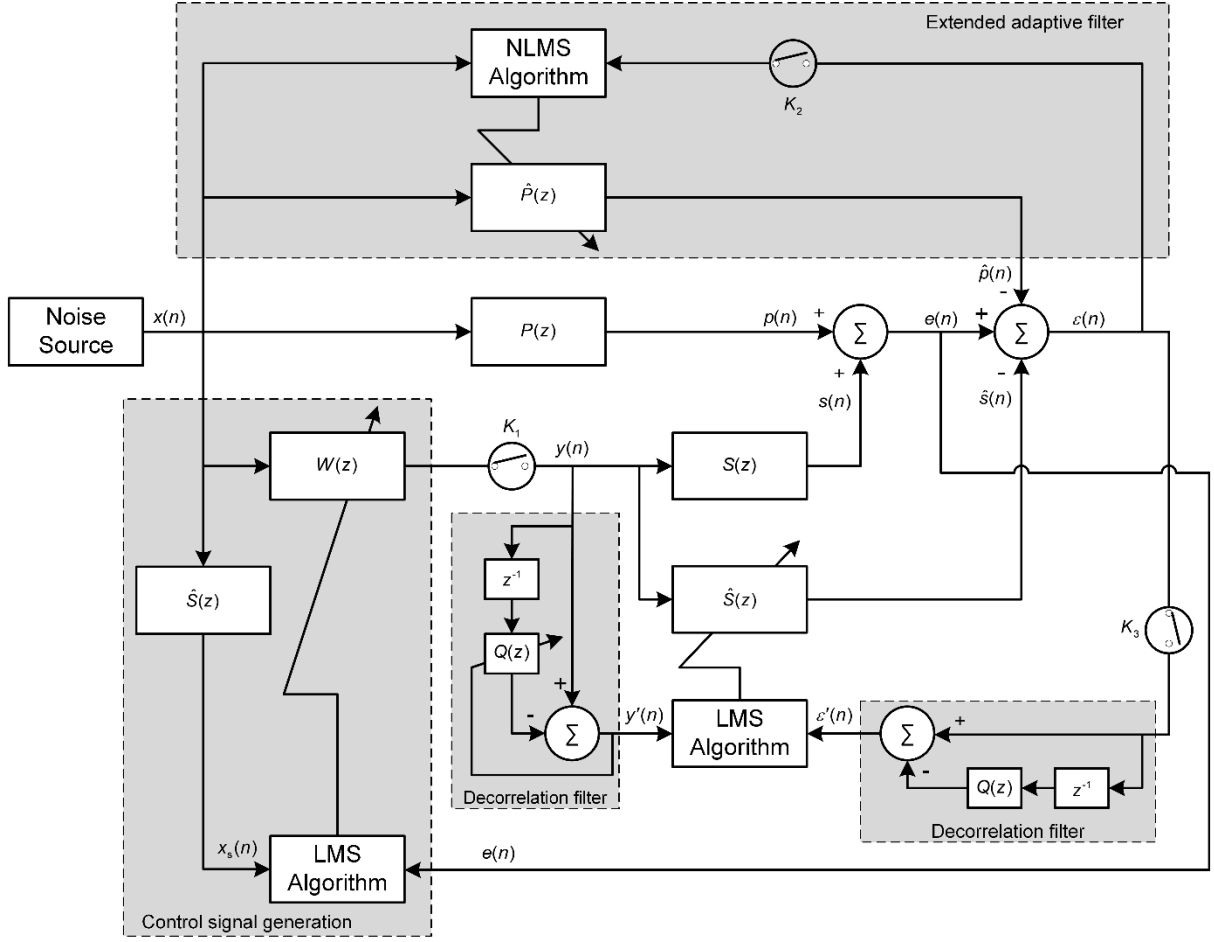
Fig. 1: Block diagram of the proposed method for active control operation.

In the second stage, K_1 is turned on and K_2 and K_3 are turned off for controller initialization. An initial controller with a single gain G is set for ANC operation, i.e., $W(z) = G$. The gain is tuned in such a way that the amplitude of the error signal $e(n)$ is higher than that of $p(n)$. In the process, the initial controller G is increased from a small pre-defined value (for example, $G = 1\%$ of the maximal gain can be applied on the system) by 2 times each step until $\sigma_e^2 > \sigma_p^2$, where σ_e^2 is the power of the error signal $e(n)$, which can be estimated by

$$\sigma_e^2(n) = \lambda \sigma_e^2(n-1) + (1-\lambda)e^2(n) \tag{2}$$

where λ is the forgetting factor ($0.9 < \lambda < 1$), σ_p^2 is the power of the primary disturbance, which can be estimated before controller initialization similarly with Eq. (2) by turning off the controller with K_1.
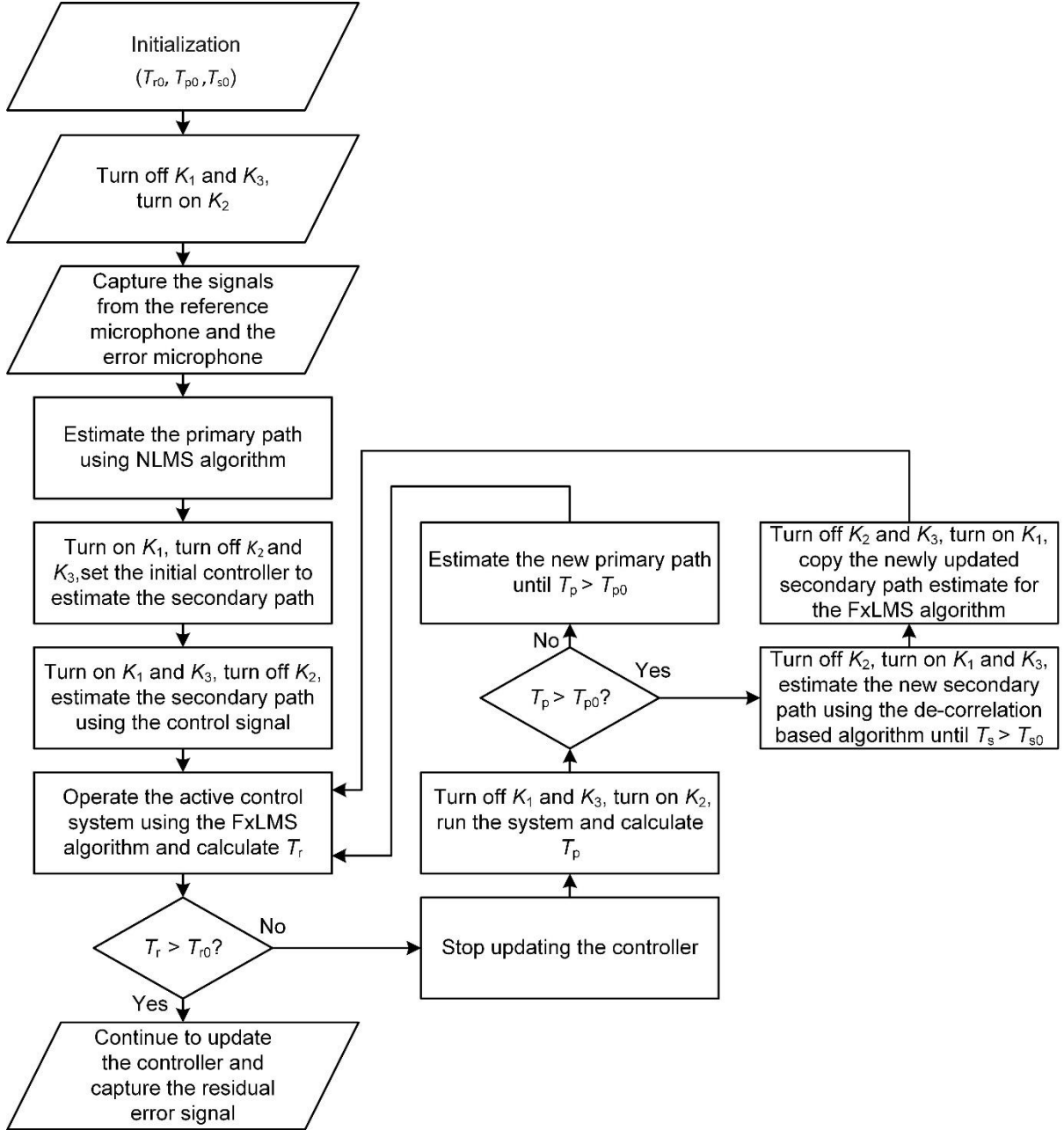
Fig. 2 Flowchart of the proposed method

The third stage involves the estimation of the secondary path $S(z)$ using the control signal, for which K_1 and K_3 are turned on, and K_2 is turned off. The control signal $y(n) = Gx(n)$ is used as the excitation signal for estimating the secondary path. In this case, the primary signal $p(n)$ acts as an interference signal in the estimation process, so the filter $\hat{P}(z)$ (estimated in the first stage) is used to remove this interference. The final error signal $\varepsilon(n) = p(n) + s(n) - \hat{s}(n) - \hat{p}(n)$ is used in the update rule given by

$$\hat{\mathbf{s}}(n+1) = \hat{\mathbf{s}}(n) + \mu_s \varepsilon(n) \mathbf{y}(n) \tag{3}$$

where $\mathbf{y}(n) = [y(n), y(n-1), \ldots, \quad y(n-L_s+1)]^T$ is the L_s sample control signal vector, μ_s is the step size. Hence, a bias free estimation of $S(z)$ is possible. If $y(n)$ is a coloured signal, the modelling may be improved by incorporating pre-whitening filters.

The fourth stage is for the complete active control operation. After obtaining the initial $\hat{P}(z)$ and $\hat{S}(z)$, the switches K_2 and K_3 are turned off, and K_1 is turned on. This means there is no update for $\hat{P}(z)$ and $\hat{S}(z)$, and the FxLMS algorithm is used for ANC operation. The control weights are updated as

$$\mathbf{w}(n+1) = \mathbf{w}(n) - \mu_w e(n)\mathbf{x}_s(n) \tag{4}$$

where $\mathbf{x}_s(n) = [x_s(n), x_s(n-1), \ldots, \quad x_s(n-L_w+1)]^T$, $x_s(n)$ is the reference signal $x(n)$ filtered through the secondary path estimate $\hat{\mathbf{s}}(n)$ and μ_w is the step size.

The active control operation is prone to acoustic path change. To detect which path changes, three thresholds are defined.

$$T_r = 10\log_{10}\left[\frac{\sigma_p^2}{\sigma_e^2}\right] \tag{5}$$

$$T_p = 10\log_{10}\left[\frac{\sigma_e^2}{\sigma_\varepsilon^2}\right] \tag{6}$$

$$T_s = 10\log_{10}\left[\frac{\sigma_{e'}^2}{\sigma_\varepsilon^2}\right] \tag{7}$$

T_r is the threshold to detect sudden rise in the residual error signal $e(n)$, T_p and T_s are the thresholds to detect if the estimated acoustic paths are accurate, $\sigma_{e'}^2$ is the power of the error signal $e'(n) = e(n) - \hat{p}(n)$ during secondary path modelling.

Assume that the normal noise reduction is 10 dB for the system, i.e., $T_{r0} = 10$, and if suddenly it becomes less than 10 dB, i.e., $T_r < 10$ dB, there should be an acoustic path change, which may come from the primary path or the secondary path or $x(n)$, the update for $W(z)$ is ceased. To check whether the change is due to the primary path, K_1 and K_3 are turned off, K_2 is turned on, and the threshold T_p is checked. Assume that normal acoustic path modelling accuracy is 20 dB for the system, i.e., $T_{p0} = 20$, and if it becomes less than 20 dB, i.e., $T_p < 20$ dB, it is confirmed that the preciously estimated acoustic path is no more matching with the changed acoustic path.

For $T_p < 20$, it is confirmed that there is a change in the primary path. Hence, $\hat{P}(z)$ is updated until the condition $T_p > 20$ is met, and then the FxLMS algorithm is used for ANC operation. If the condition $T_p > 20$ is valid, the change in $e(n)$ might be due to the change in secondary

path. To update $\hat{S}(z)$, K_2 is turned off and K_1 and K_3 are turned on. The secondary path modelling is carried out until the condition $T_s > T_{s0}$ is met with the previously obtained $W(z)$. The normal secondary path modelling accuracy can be assumed to be 20 dB, i.e., $T_{s0} = 20$.

Decorrelation filters are widely employed for adaptive filtering application such as feedback cancellation in hearing aids [14]. However, they have little application in active control operation. Two identical adaptive decorrelation filters $D(z)=1-z^{-1}Q(z)$ are introduced to accelerate the convergence behaviour of the secondary path modelling process, where $Q(z)$ is the z-transform of $\mathbf{q}(n) = [q_0(n), q_1(n), \dots, q_{M-1}(n)]^T$ with M representing the tap-weight length of $Q(z)$ [15, 16]. The signal $y(n)$ passes through the adaptive decorrelation filter to provide the signal $y'(n) = y(n) - \mathbf{q}^T(n)\mathbf{y}_1(n)$, where $\mathbf{y}_1(n) = [y(n-1), y(n-2), \dots, y(n-M)]^T$. Similarly, the error signal $\varepsilon(n)$ passes through the decorrelation filter to provide $\varepsilon'(n) = \varepsilon(n) - \mathbf{q}^T(n)\boldsymbol{\varepsilon}_1(n)$, where $\boldsymbol{\varepsilon}_1(n) = [\varepsilon(n-1), \varepsilon(n-2), \dots, \varepsilon(n-M)]^T$. The signals $y'(n)$ and $\varepsilon'(n)$ are used to update the filter $S(z)$. The decorrelation filter can pre-whiten the updating signals y(n) and the error signal $\varepsilon(n)$, which in turn accelerates the convergence of $S(z)$. The adaptive decorrelation filters is updated using the NLMS algorithm as

$$\mathbf{q}(n+1) = \mathbf{q}(n) + \mu_q \frac{y'(n)\mathbf{y}_1(n)}{\mathbf{y}_1^T(n)\mathbf{y}_1(n)} \tag{8}$$

The tap-weights of the of $S(z)$ are updates as

$$\hat{\mathbf{s}}(n+1) = \hat{\mathbf{s}}(n) + \mu_s \varepsilon'(n)\mathbf{y}'(n) \tag{9}$$

where $\mathbf{y}'(n)=[\, y'(n),\, y'(n-1), \dots, y'(n-L_s+1)]^T$.

After obtaining $S(z)$, K_2 and K_3 are turned off, K_1 is turned on, the new secondary path estimate is used in the FxLMS algorithm for active control operation by updating the control coefficients as in (4). The stages involved in the proposed method are summarized in Table I.

Table I: The 5 stages of the proposed method.

Stage 1: Primary path estimation
Turn off K_1 and K_3, turn on K_2
Estimate of the primary path $\hat{P}(z)$
$\mathbf{p}(n+1) = \mathbf{p}(n) + \mu_p \dfrac{\varepsilon_p(n)\mathbf{x}_p(n)}{\mathbf{x}_p^T(n)\mathbf{x}_p(n)}$
Stage 2: Controller initialization

Turn on K_1, turn off K_2 and K_3

Set the initial controller

Stage 3: Secondary path estimation

Turn on K_1 and K_3, turn off K_2

Estimate of the secondary path $\hat{S}(z)$ using control signal

$$\hat{\mathbf{s}}(n+1) = \hat{\mathbf{s}}(n) + \mu_s \varepsilon(n)\mathbf{y}(n)$$

Stage 4: Primary and secondary path changing detection in active control operation

Operate the active control system

$$\mathbf{w}(n+1) = \mathbf{w}(n) - \mu_w e(n)\mathbf{x}_s(n)$$

if $T_r < T_{r0}$, A path change is detected.

To check primary path change, turn off K_1 and K_3, turn on K_2, run the system

if $T_p < T_{p0}$, update $\hat{P}(z)$.

else, turn on K_1 and K_3, turn off K_2, update $\hat{S}(z)$ using

$$\mathbf{q}(n+1) = \mathbf{q}(n) + \mu_q \frac{y'(n)\mathbf{y}_1(n)}{\mathbf{y}_1^T(n)\mathbf{y}_1(n)}$$

$$\hat{\mathbf{s}}(n+1) = \hat{\mathbf{s}}(n) + \mu_s \varepsilon'(n)\mathbf{y}'(n)$$

Stage 5: Active control operation

Turn off K_2 and K_3, turn on K_1

Operate the active control system with updated $\hat{S}(z)$

If rise in $e(n)$ is detected, follow the procedures of Stage 4

3. Computational Complexity

A detailed computational complexity of the proposed method is computed in this section. The proposed method requires L_w multiplications and $L_w - 1$ additions to obtain the controller output; L_s multiplications and $L_s - 1$ additions to obtain the filtered reference signal; L_s multiplications and $L_s - 1$ additions to obtain the estimated cancelling signal; L_p multiplications and $L_p - 1$ additions to obtain the output of extended adaptive filter; $2M$ multiplications and $2(M - 1)$ additions to obtain the decorrelation filter outputs; $L_w + 1$ multiplications and L_w additions to update the control filter; $2L_p + 1$ multiplications, $2L_p - 1$ additions and 1 division to update the extended adaptive filter $\hat{P}(z)$; $L_s + 1$ multiplications and

L_s additions to update the secondary path modelling filter; $2M + 1$ multiplications, $2M - 1$ additions and 1 division for updating the decorrelation filter. For calculating the thresholds, 6 multiplications, 6 additions, 3 divisions and 3 logarithmic operations are required. The proposed method may requires a total of $2L_w + 3L_s + 3L_p + 4M + 10$ multiplications, $2L_w + 3L_s + 3L_p + 4M - 2$ additions, 5 divisions and 3 logarithmic operations. Hence, $4L_w + 6L_s + 6L_p + 8M + 16$ computations are required per sample. However, it is to be noted that the secondary path modelling and control operation are not carried out simultaneously, which may lead to a reduced computational complexity than the above mentioned values.

For the sake of comparison, the computational complexity of some existing approaches is summarized in Table II, which includes the extended filtering method in [10], conventional extended filtering method [18], Yang's method [6], Carini's method [8] and Gao's method [13]. To make a straightforward comparison, one example is provided, where L_w= 48, L_s= 16, L_p=48, M= 5, and for Gao's method, the length of the prototype filter K_L=128, the down sampling rate N_D=10, the number of total subband N_t=20, the number of actual used subband N_a=4, direct path delay Δ=17, length of Hilbert filter L=34. The details of the computational complexity of Gao's method can be found in [13]. It can be observed from Table II that the computational complexity of the proposed method is higher than that of the the extended filtering methods and Yang's method. However, it is lesser compared to that of Carini's and Gao's method.

Table II: Computational complexity of different methods

Methods	Total computations per sample	Example
Proposed Method	$4L_w + 6L_s + 6L_p + 8M + 16$	632
extended filtering [10]	$4L_w + 6L_s + 2L_p - 4$	380
extended filtering [18]	$4L_w + 6L_s + 6L_p$	576
Yang's Method [6]	$4L_w + 6L_s + 4L_h + 24$	344
Carini's Method [8]	$13L_w + 12L_s + 8D + 25$	905
Gao's Method [13]	$L_w + L + \Delta + \dfrac{N_a(2L_w + 1)}{N_D}$ $+ \dfrac{3(K_L + N_t\log_2 N_t)}{N_D}$ $+ N_a(10 + 8L_w)$	1778

4. Simulations

In the simulations, the primary path $P(z)$ and secondary path $S(z)$ are FIR filters of length 48 and 16 respectively which are obtained from the data provided in [17], the frequency response of which are depicted in Fig. 3. Part A represents the normal paths, Part B represents the path after a sudden change. The estimated secondary path and control filter are FIR filters of length $L_s = 16$ and $L_w = 48$, respectively. The adaptive decorrelation filter $Q(z)$ is an FIR filter of length $M = 5$. The sampling frequency used in the simulation is 2000 Hz.
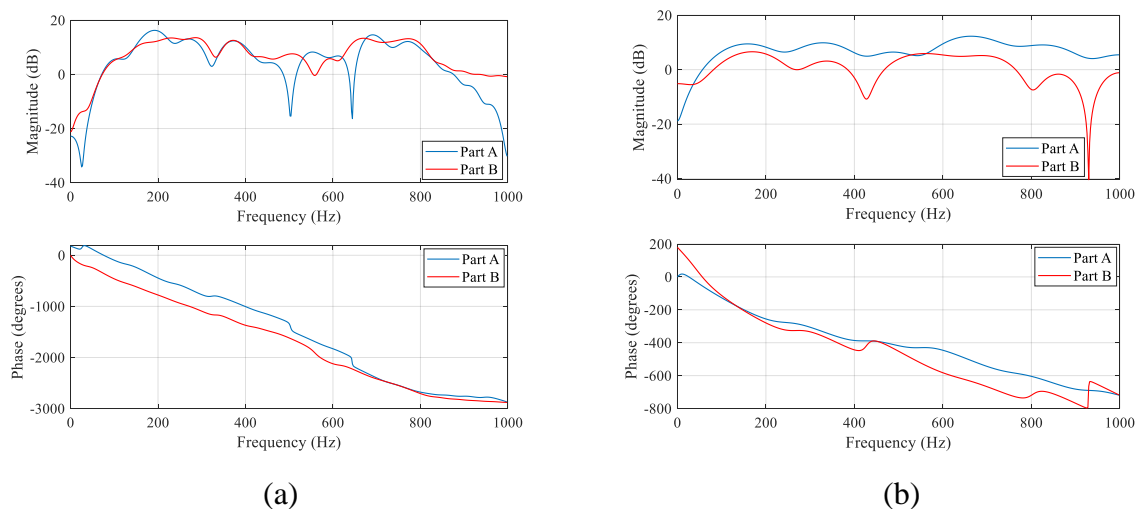

Fig. 3 Frequency response of (a) the primary path and (b) the secondary path.

The mean square error (MSE) and the relative modelling error ΔS are used as the metrics for comparison, which are defined as

$$\text{MSE} = 10\log_{10}\left\{E\left[e^2(n)\right]\right\} \tag{10}$$

$$\Delta S \ (\text{dB}) = 10\log_{10}\left\{\frac{\|\mathbf{s}(n) - \hat{\mathbf{s}}(n)\|^2}{\|\mathbf{s}(n)\|^2}\right\}. \tag{11}$$

Simulations have been carried out to compare the performance of the proposed 5-stage method with the extended filtering (EF) method reported in [10], which is hereafter referred to as EF-1, the conventional extended adaptive filter method [18], which is hereafter referred to as EF-2, Carini's method [6] and Yang's method [8]. In EF-1, the extended filter is the estimate of the primary path, which is fixed for control operation, whereas the extended filter is adaptive one for EF-2. Both Carini's method and Yang's method use auxiliary noise with an initialized variance of 0.05 and power scheduling strategy for simultaneous update of the control filter

and secondary path modelling filter. All the results obtained are averaged over ten independent trials.

4.1 The 5-stage method

In this subsection, simulation has been carried out for different situations to test the efficacy of the 5-stage method for both the primary and the secondary path change.

4.1.1 Case 1

In this case, the input signal $x(n)$ is generated from a first order autoregressive process

$$x(n) = 0.9x(n-1) + v(n) \tag{12}$$

where $v(n)$ is a white noise of zero mean and unit variance. A white Gaussian measurement noise with a signal to noise ratio (SNR) of 40 dB is considered. The simulation runs for 50 sec and suddenly both the primary and secondary paths are changed (Part B). The simulation parameters used for the proposed method are: $\mu_p = 0.5$, $\mu_s = 0.004$, $\mu_w = 0.0001$, and for the EF methods are: $\mu_p = 0.008$, $\mu_s = 0.02$, $\mu_w = 0.0001$. The simulation parameters used for the Yang's method are: $\mu_w = 0.000005$, $\alpha = 0.02$ and $\mu_h = 0.003$, $c = 1$, $\lambda = 0.999$, and for the Carini's method are: $\mu_{s_{min}} = 0.001$, delay $D = 8$, $\hat{\lambda} = 0.8$, $R = 1$. The step sizes and other simulation parameters are chosen by trial and error to keep the system stability for normal acoustic paths and yet with the best possible control performance.

The learning curves are shown in Fig. 4. The proposed method maintains the control after both the primary and the secondary path change, while the EF-1 and EF-2 algorithms diverge. The Yang's method and Carini's method are also able to maintain the control operation before and after the acoustic path change. However, the control performance is limited compared to the proposed method. It is due to the fact that the control operation and secondary path modelling process interfere with each other, and the injected auxiliary noise in these two methods affect the residual noise level. Furthermore, it is to be noted that the initial residual error levels (Part A) of Yang's method and Carini's method are higher compared to the other methods due the injection of auxiliary noise. For the proposed algorithm, after the detection of the path change at 50th second, the controller update is ceased, K_1 and K_3 are turned off, K_2 is turned on, and the primary path is remodelled. Hence, the residual error becomes exactly same as the primary disturbance during that time, which is clear from the learning curve (50th-60th second). During the secondary path modelling, K_1 and K_3 are turned on, K_2 is turned off, the controller preserves the previously updated coefficients (60th-70th second). After the

modelling of the acoustic paths are completed, K_2 and K_3 are turned off, K_1 is turned on, the controller is continued to update to reduce residual noise.

For Part A, the proposed method, EF-1 and EF-2 are able to reach same residual noise level of approximately -11.5 dB, where as the Yang's method and Carini's method are capable of achieving -7.5 dB despite having the fact that the convergence behaviour of the Yang's method is the worst among the methods under study. After acoustic path change, the achieved residual noise levels for the proposed method, Yang's method and Carini's method are -11 dB, 2 dB and -0.07 dB, respectively. The improved performance of the Carini's method (among Yang's method and Carini's method) might be attributed to the use of optimal varible step size for control filter update and secondary path modelling and appropriate auxiliary noise power scheduling.
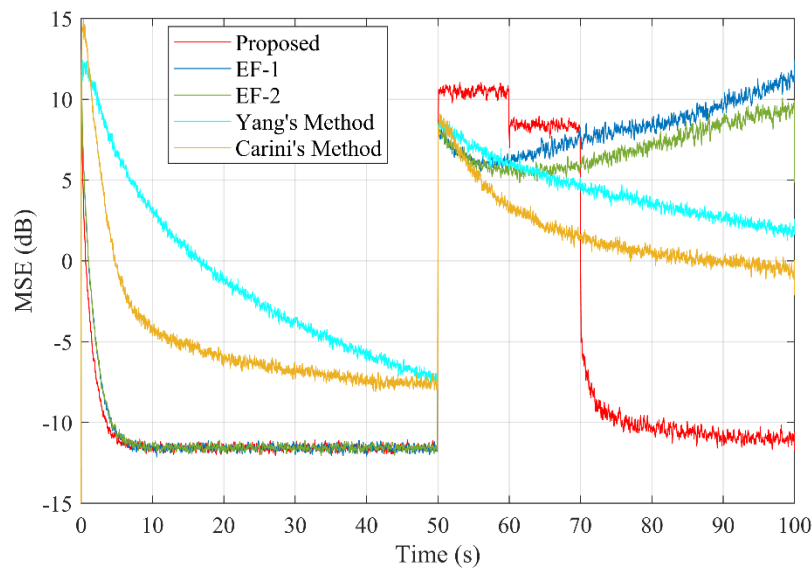

Fig. 4: Case 1: Learning curve for the 5-stage method obtained from an AR(1) input signal.

The deterioration in performance for the EF methods after both the primary and the secondary path change is due to the fact that it is not capable of estimating the changed paths accurately. It is found that the phase error between the actual and estimated secondary path for the EF-1 and EF-2 methods is greater than ±90°, thereby making both the algorithms diverge. Furthermore, in the simultaneous update of secondary path estimation filter and the control filter, both the processes interfere with each other. An inaccurate secondary path estimation filter leads to increased interferences in control operation.

4.1.2 Case 2

In this case, a more critical scenario is considered, where both the primary and secondary paths change frequently. The input signal is same as Case 1. The simulation runs for 25 seconds with normal acoustic paths (Part A), and then both the paths are changed (Part B). The acoustic paths again changes to Part A and Part B at 50th and 75th second, respectively. The simulation parameters used for this case are: the proposed method ($\mu_p = 0.5$, $\mu_s = 0.004$, $\mu_w = 0.0001$), the EF methods ($\mu_p = 0.0005$, $\mu_s = 0.001$, $\mu_w = 0.0001$), Yang's method ($\mu_w = 0.000005$, $\alpha=0.02$ and $\mu_h=0.003$, $c=1$, $\lambda=0.999$) and Carini's method ($\mu_{s_{min}} = 0.001$, delay $D=8$, $\hat{\lambda}=0.8$, $R=1$). The step sizes are chosen by trial and error to have same initial convergence (the proposed method and EF methods), and stability of all the methods for the normal acoustic paths. The operation of the switches are same as Case 1. The learning curves are shown in Fig. 5, which shows the superiority of the proposed method after sudden path change. The EF-1 and EF-2 algorithms diverge after the acoustic path change for the same reason as Case 1. Though the Yang's method and Carini's method offer control operation after each path change, their control performance is limited due to the simultaneous update of control filter and secondary path modelling filter and the existence of auxiliary noise in the residual error signal.
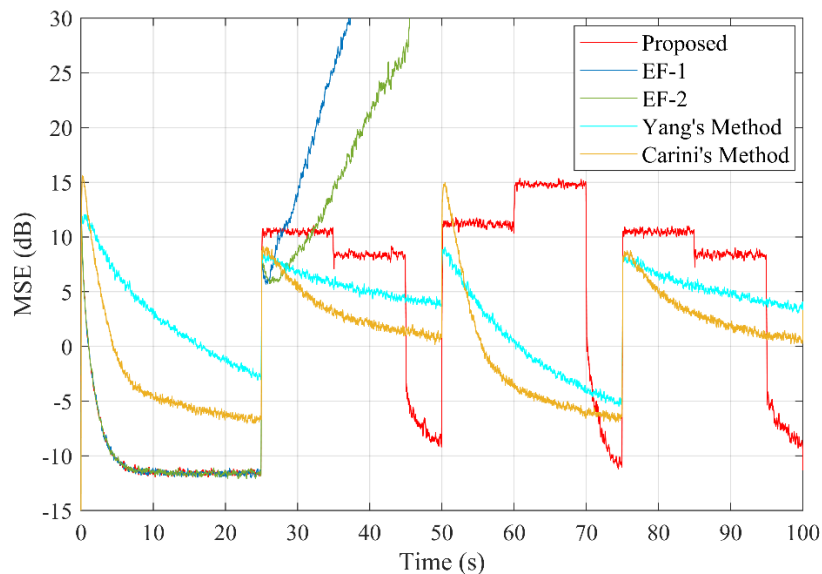

Fig. 5: Case 2: Learning curve for the 5-stage method obtained from an AR(1) input signal with a frequent acoustic path change.

For normal acoustic path (Part A), the proposed method, EF-1 and EF-2 are able to reach the same residual noise level (that is around -11.5 dB), whereas the Yang's method and the

Carini's method achieves -2.8 dB and -6.5 dB, respectively. The residual noise levels for the proposed method, the Yang's method and the Carini's method for the first acoustic path change are -9 dB, 4 dB and 1dB, respectively, while such obtained values for the second path change are -10.8 dB, -5 dB and -6.5 dB, respectively. Also, the third acoustic path change offers -9.5 dB, 3.5 dB and 0.9 dB, respectively, for such three mentioned methods.

One can observe from the results that the proposed method is able to achieve similar level of noise reduction only after remodelling the acoustic paths. The primary path modelling is carried out during 25th-35th second, 50th-60th second and 75th-85th second. Similarly, the secondary path modelling is carried out during 35th-45th second, 60th-70th second and 85th-95th second. The remodelling process took longer time compared to the controller update duration, which means the unwanted disturbance is present for a long time. Hence, it is expected that the time duration for remodelling the acoustic paths could be shorter compared to the time gap between two consecutive path changes. This may be achieved by accelerating the convergence behaviour of the adaptive filters used for modelling. The adaptive decorrelation filters are introduced in Section 4.2 to reduce the modelling time.

There might be some situations where only one acoustic path changes. If $T_r < T_{r0}$, the controller is ceased, K_1 and K_3 are turned off, K_2 is turned on. If $T_p < T_{p0}$, it confirms the need for remodelling of the primary path. However, the remodelling of primary path takes some time. After the remodelling is completed, the controller update is continued, which means the convergence of the FxLMS algorithm in such a case depends on the primary path remodelling time. Similarly, if $T_r < T_{r0}$, and $T_p > T_{p0}$, it confirms the need for remodelling of the secondary path, for which K_1 and K_3 are turned on and K_2 is turned off. The controller update is continued after remodelling of the secondary path, which means the convergence of the FxLMS algorithm in such a case depends on the secondary path remodelling time.

In summary, the proposed 5-stage method is capable of maintaining the noise reduction performance even both the primary and the secondary path change. However, one weakness of this method is that it takes some time for remodelling the acoustic paths, which makes it ill-suited for the situation where the changes in the acoustic paths occur more frequently before one remodelling is completed.

4.2 The Decorrelation filter

In this subsection, the advantages of using the adaptive decorrelation filter is illustrated through simulations. For applying the decorrelation filter for modelling the secondary path (Part B), the

modelling signal used is the controller output signal from Part A. After the confirmation of secondary path change, K_1 and K_3 are turned on, K_2 is turned off, the controller preserves the previously updated coefficients (from Part A). Please note that this decorrelation filter is not effective for tonal and white excitation signal.

4.2.1 Case 1

The input signal and other simulation parameters are same as the Case 1 of previous section. The step size used for updating the coefficients of the decorrelation filter is $\mu_q = 0.01$. It is evident from Fig. 6 that the decorrelation filter accelerates the convergence behaviour of the secondary path modelling filter. Unlike the conventional LMS adaptive filter, the decorrelation adaptive filter takes approximately 2 second to achieve similar modelling accuracy. That means the use of adaptive decorrelation filter can reduce the overall modelling time. The improvement in the convergence behaviour of the decorrelation adaptive filter is due to its pre-whitening operation, which decreases the spectral dynamic range of the excitation signal used for modelling.
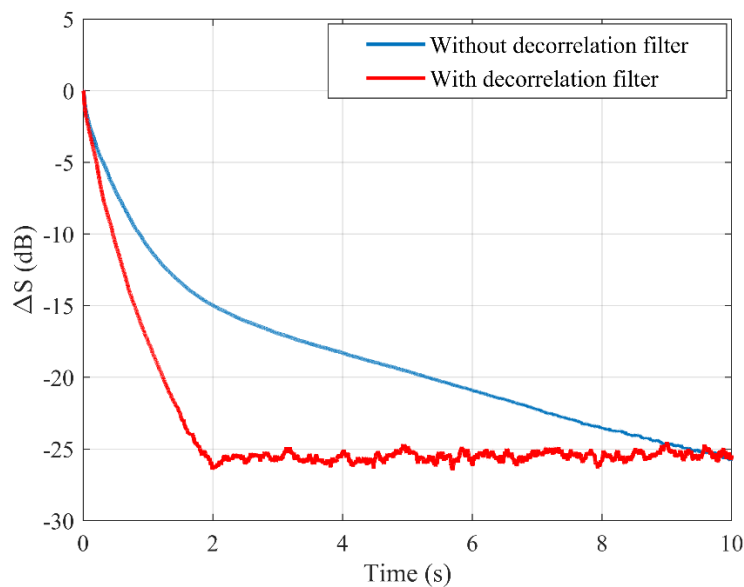

Fig. 6: Relative modelling error for the AR(1) signal.

4.2.2 Case 2

A broadband reference noise signal is considered in this case. A 21 order FIR filter with a pass band of [100 500] Hz is designed using *fir1* command. A white noise of zero mean and unit variance is filtered through this bandpass filter to generate the reference signal $x(n)$. A white

Gaussian measurement noise with an SNR of 40 dB is considered. The acoustic paths used in the simulation are shown in Fig. 3. The control operation is carried out for Part A and the acoustic paths are changed suddenly (Part B). The decorrelation adaptive filter is used for remodelling the secondary path. The simulation parameters used for the proposed method are: $\mu_p = 0.9$, $\mu_s = 0.01$, $\mu_w = 0.00005$ and $\mu_q = 0.01$.

The relative modelling error is shown in Fig. 7(a), from which one can notice that the proposed decorrelation filter is improving the modelling accuracy by approximately 3 dB. The adaptive filter without the decorrelation filter takes 10 second to achieve approximately -4 dB modelling error, while the decorrelation adaptive filter reaches the same level at around 2 second. The reason for such improvement is explained in the previous case. In this case, the reference signal has bandwidth [100 500] Hz, and the secondary path can be modelled accurately only in that band. Fig. 7 (b) shows the modelling error in the frequency band of the reference signal, from which it is clear that the modelling is improved using the decorrelation filter. The modelling error in Fig .7(a) is higher compared to the previous case as it is obtained by considering the whole range of frequency response of the secondary path. However, the condition $T_s > T_{s0}$ is met.
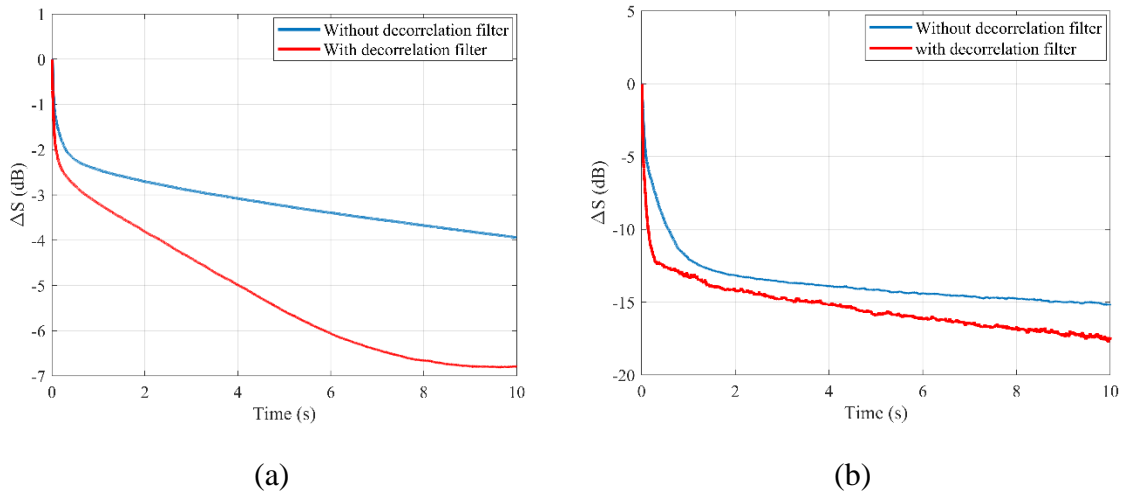

(a)   (b)

Fig. 7: (a) Relative modelling error for the full frequency range, (b) Relative modelling error for the frequency band of [100 500] Hz.

4.2.3 Case 3

In this case, the reference signal is a mixture of white noise with zero mean and unit variance and multitone signal comprising frequencies of 100, 200, 300, 400 and 500 Hz. The variance of the multitone signal is adjusted to 2. A white Gaussian measurement noise with an SNR of

40 dB is considered. The acoustic paths used in the simulation are shown in Fig. 3. The control operation is carried out for Part A and the acoustic paths are changed suddenly (Part B). The decorrelation adaptive filter is used for remodelling the secondary path. The simulation parameters used for the proposed method are : $\mu_p = 0.9$, $\mu_s = 0.003$, $\mu_w = 0.0002$ and $\mu_q = 0.004$.

The relative modelling error is illustrated in Fig. 8, from which it is clear that the decorrelation filter accelerates the convergence speed of the secondary path modelling filter. Although the reference signal constitutes white noise, the presence of the control filter makes the output of controller as a correlated (coloured) signal, increasing the spectral dynamic range. The adaptive decorrelation filter, in such a case, improves the convergence speed. It is to be noted that if the controller output, the excitation signal for modelling the secondary path is white or tonal, the decorrelation filter is not more effective than that without using the decorrelation filter for modelling the secondary path.
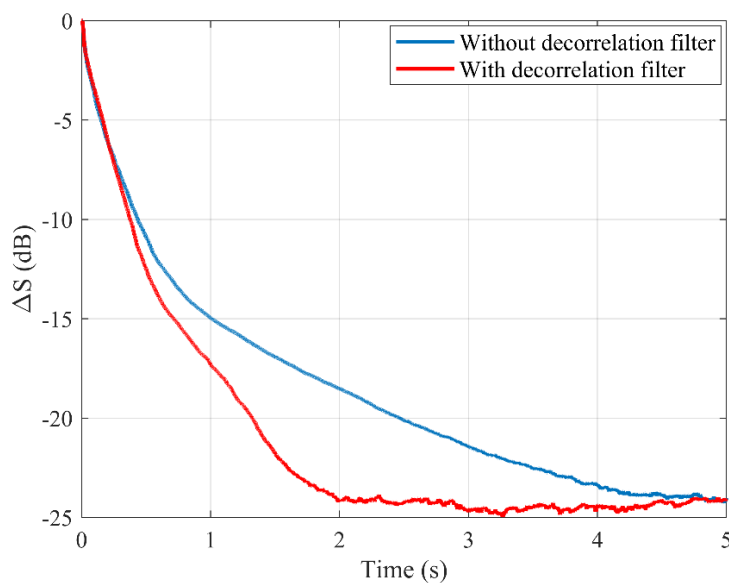

Fig. 8: Relative modelling error for the mixture of white noise and multitone signal.

In summary, although the decorrelation filter is not effective to increase the convergence speed for tonal and white excitation signals, it can accelerate the convergence speed of the secondary path modelling for broadband and narrowband signals. Even though the reference signal might be white noise, the presence of the control filter, the frequency response of which is not flat in general, converts a white reference input signal to a coloured excitation signal for the secondary path modelling, which makes the decorrelation filter become effective. The effectiveness decreases with the reduction of bandwidth of the excitation signal. The order of

the decorrelation filter also plays a role in improving the convergence speed. In the simulations, a small order filter is considered. However, a higher order filter may be chosen for complicated coloured signals.

4.3 The 5-stage method with decorrelation filter

In this subsection, the complete ANC operation is carried out, which includes the proposed 5-stage method and the adaptive decorrelation filter. Three cases have been considered here.

4.3.1 Case 1

The input signal considered in this case is a coloured signal, generated by passing a white noise with zero mean and unit variance through a filter $(1 + 0.5z^{-1} + 0.81z^{-2})/(1 - 0.59z^{-1} + 0.4z^{-2})$. A white Gaussian measurement noise with an SNR of 40 dB is considered. The acoustic paths considered are depicted in Fig. 3. The simulation is carried out with normal acoustic paths (Part A), then there is a sudden change in both the acoustic paths at 40th second. The operation of the switches for remodelling of acoustic paths and control operation are same as previous cases. The simulation parameters used for this case are: the proposed method (μ_p = 0.5, μ_s = 0.004, μ_w = 0.0001, μ_q = 0.5), the EF methods (μ_p = 0.01, μ_s = 0.004, μ_w = 0.0001), Yang's method (μ_w = 0.000005, α=0.02 and μ_h=0.003, c=1, λ=0.999) and Carini's method ($\mu_{s_{min}}$ = 0.06, delay D=8, $\hat{\lambda}$=0.9, R=1).

In the proposed method, the primary path modelling is carried out during 40th-50th second. After the detection of secondary path change, K_2 is turned off, K_1 and K_3 are turned on. The secondary path modelling can be completed earlier using the decorrelation filter because the controller output signal is coloured. The adaptive decorrelation filter reduces the spectral dynamic range of the control signal, there by improves the convergence speed of the modelling filter. Unlike the LMS adaptive filters, the decorrelation adaptive filter takes approximately 2 second (50th-52nd second) data samples for the secondary path modelling. The learning curves of the system are shown in Fig. 9, from which it is clear that the decorrelation filter reduces the remodelling time and helps to resume the control operation. The steady-state performance with and without the decorrelation filter are similar. It is also evident that both the primary and the secondary path change cause the EF-1 and EF-2 algorithms diverge, while the proposed algorithm is able to achieve similar level of noise reduction. Yang's method and Carini's method are also capable of maintaining control operation after acoustic path change, the control performances of which are less compared to the proposed method.
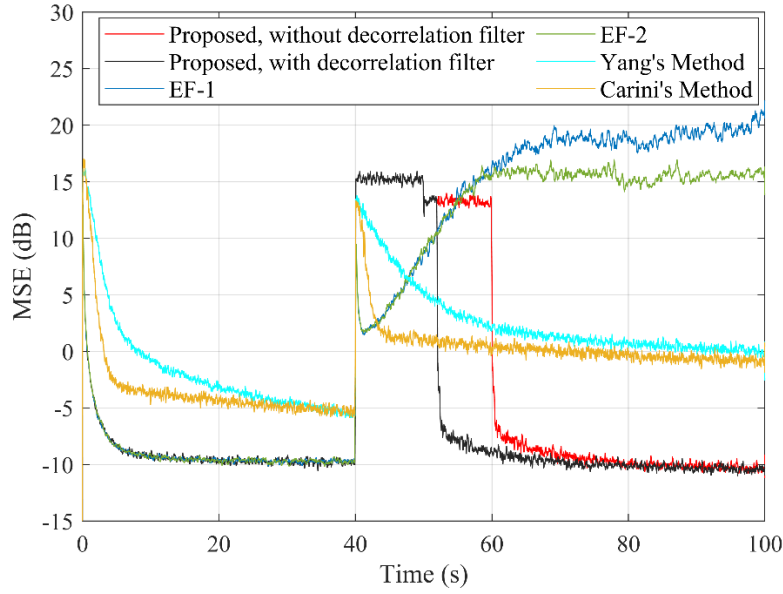
Fig. 9: Learning curve for the 5-stage method obtained from a coloured input signal.

For Part A, the proposed method (with and without decorrelation filter), EF-1 and EF-2 reach the same residual noise level, i.e., around -9.5 dB, whereas the Yang's method and the Carini's method achieves similar residual noise level, i.e., around -5.5 dB. The residual noise levels for the proposed methods, the Yang's method and the Carini's method after the acoustic path change are -10.2 dB, -0.1 dB and -0.8 dB, respectively.

4.3.2 Case 2

In this case, the input signal and other simulation parameters (for the proposed methods) are same as the Case 3 of Section 4.2. The simulation is carried out with normal acoustic paths (Part A), then there is a sudden change in both the acoustic paths at 25th second. The operation of the switches for remodelling of acoustic paths and control operation are same as previous cases. The simulation parameters used for the existing methods are: the EF methods ($\mu_p =$ 0.001, $\mu_s = 0.01$, $\mu_w = 0.0002$), Yang's method ($\mu_w = 0.00001$, $\alpha=0.07$ and $\mu_h=0.003$, $c=1$, $\lambda=0.999$) and Carini's method ($\mu_{s_{min}} = 0.02$, delay $D=8$, $\hat{\lambda}=0.9$, $R=1$).

It can be observed from the relative modelling error depicted in Fig. 8 that the decorrelation adaptive filter can remodel the secondary path earlier compared to the LMS counterpart. The primary path remodelling is carried out fast, with in one second as the reference signal constitutes a white noise. The LMS adaptive filter remodels the secondary path during 26th-31st second, while the decorrelation adaptive filter can do it in 2 second. The learning curves of the

system are shown in Fig. 10, from which it is clear that the decorrelation filter reduces the remodelling time and the control operation is maintained. The EF-1 and EF-2 algorithms diverge after both the primary and the secondary path change.

For Part A, the proposed method (with and without decorrelation filter), EF-1 and EF-2 reach the same residual noise level, i.e., around -9.3 dB, whereas the Yang's method and the Carini's method achieves similar level of residual noise, i.e., around -8 dB. The residual noise levels for the proposed methods, the Yang's method and the Carini's method after the acoustic path change are -10.5 dB, 2.4 dB and -0.5 dB, respectively. It can also be noticed from part A that the initial residual noise levels for Yang's method and Carini's method are higher than that of the other methods, which are caused by the power scheduling of the injected auxiliary noise.
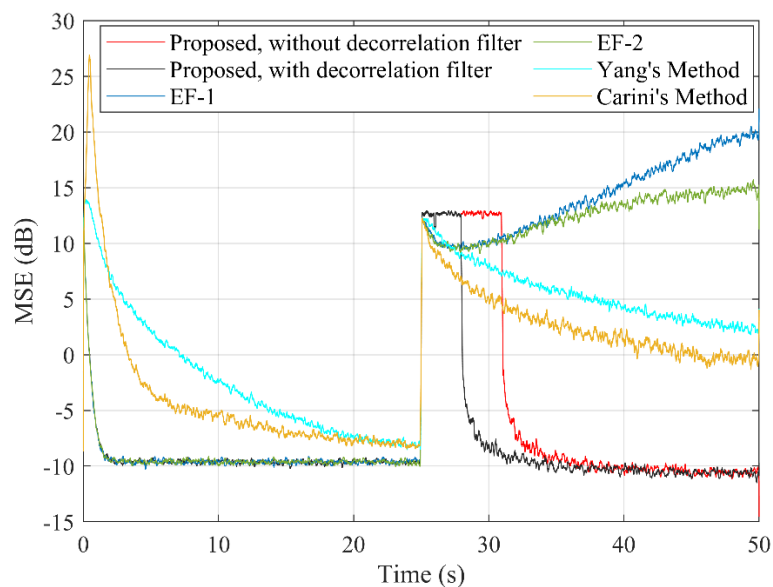

Fig. 10: Learning curve for the 5-stage method obtained from a mixture of white noise and multitone input signals.

4.3.3 Case 3

In this case, the effect of different level of measurement noise on the performance of the proposed method is investigated. The input signal, simulation condition and all other simulation parameters are same as Case 1 of Section 4.3. A white Gaussian measurement noise with four different SNR values such as 30 dB, 20 dB, 10 dB and 0 dB are considered. The obtained learning curves are depicted in Fig. 11. As it can be observed from Fig. 9 that the EF-1 and EF-2 results in algorithmic divergence after the acoustic path change, only Yang's method and Carini's method are compared with the proposed method with decorrelation filter.

The residual noise levels for Part A and Part B are shown in Table III, from which one can observe that the SNR values of 30 dB and 20 dB has little effect on the residual noise levels for the methods, but all the three methods are affected by the measurement noise of SNR values 10 dB and 0 dB. Furthermore, the proposed method outperforms the Yang's and Carini's method and achieves lower level of residual noise for all SNR values.

(a)   (b)
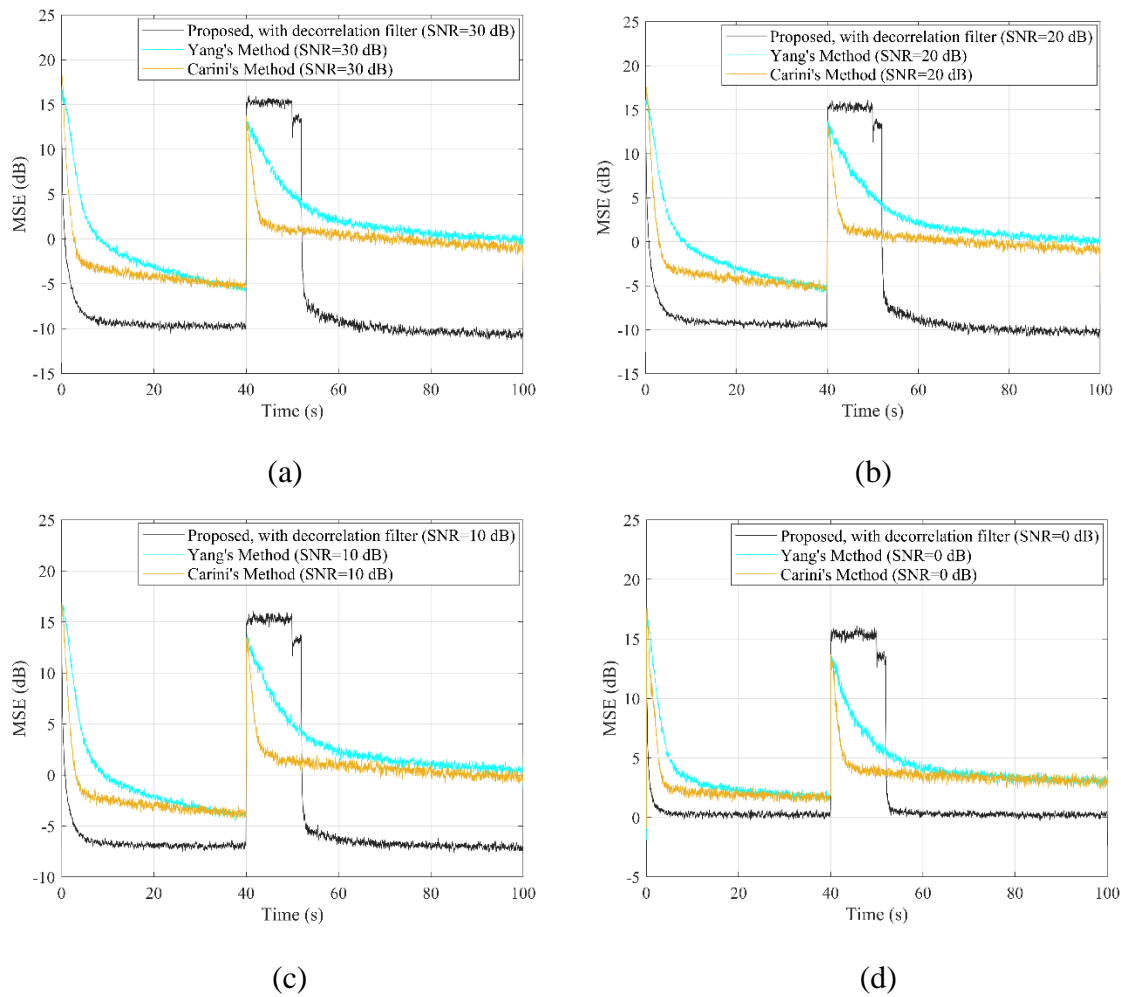
(c)   (d)

Fig. 11: Learning curves for the proposed method obtained from a coloured input signal and different level of measurement noise. (a) SNR = 30 dB, (b) SNR = 20 dB, (c) SNR = 10 dB and (d) SNR = 0 dB.

Table III: Residual noise levels of different methods for different measurement noise levels.

Residual noise level (dB)			
SNR=30 dB	SNR = 20 dB	SNR = 10 dB	SNR = 0 dB

Methods	Part A	Part B	Part A	Part B	Part A	Part B	Part A	Part B
Proposed	-9.5	-10.2	-9.2	-10.0	-6.7	-7.3	0.3	0.1
Yang's	-5.4	-0.1	-5.2	0.0	-3.8	0.6	1.9	3.0
Carini's	-5.0	-0.8	-5.0	-0.7	-3.8	0.0	1.8	3.0

In summary, the proposed 5-stage method and the decorrelation filter maintain the control operation when both the primary and the secondary path change. Unlike the existing algorithms, the proposed method detects the change of acoustic paths by monitoring the pre-set thresholds, and then uses three switches for choosing the active control operation, remodelling the primary path and remodelling the secondary path. It removes the primary disturbance during secondary path modelling, reduces the convergence time of the control filter by reducing the remodelling time of the secondary path modelling filter with the decorrelation filter. The proposed method possesses larger computational complexity than the EF-1, the EF-2 algorithms and Yang's method due to the threshold detections, the presence of two identical decorrelation filters, the coefficient update of the decorrelation filters and obtaining the pre-whitened signals. Furthermore, the remodelling of the acoustic paths requires few seconds. The price paid for the improved performance is the increased computational load. The proposed method is also robust enough to handle higher level of measurement noise. Although the proposed method can be useful for narrowband and broadband signals for handling both the primary and the secondary path change, it may not provide significant improvement in performance in situations where the excitation signal is tonal or white and the changes in the acoustic paths occur more frequently before one remodelling is completed.

5. Conclusion

A five-stage systematic method is proposed for practical active control operation which can maintain control when both the primary and the secondary path change. To improve the convergence speed of the secondary path modelling with the control signal, adaptive decorrelation filters are incorporated in the online secondary path modelling by pre-whitening the modelling signals used in the modelling. Simulation study reveals that the proposed method outperforms the conventional extended adaptive filtering methods in terms of convergence rate and stability, and outperforms Yang's method and Carini's method in terms of noise reduction. However, the proposed 5-stage method is ill-suited for the situation where the changes in the

acoustic paths occur more frequently before one remodelling is completed. Although the decorrelation filter reduces the modelling time of the secondary path modelling for broadband and narrowband signals, it is not effective for tonal and white excitation signals. Future work includes applying the variable-tap-length algorithm to find the optimum number of decorrelation filter coefficients necessary to pre-whiten complicated coloured signals, which in turn can reduce the computational complexity imposed by the use of the decorrelation filters.

Role of the funding source

References

[1]   S. Elliott, *Signal processing for active control*. Elsevier, 2000.

[2]   N. Saito and T. Sone, "Influence of modeling error on noise reduction performance of active noise control systems using filtered-x LMS algorithm," *Journal of the Acoustical Society of Japan (E),* vol. 17, no. 4, pp. 195-202, 1996.

[3]   C. Hansen, S. Snyder, X. Qiu, L. Brooks, and D. Moreau, *Active control of noise and vibration*. CRC press, 2012.

[4]   L. J. Eriksson and M. C. Allie, "Use of random noise for on-line transducer modeling in an adaptive active attenuation system," *The Journal of the Acoustical Society of America,* vol. 85, no. 2, pp. 797-802, 1989.

[5]   M. T. Akhtar, M. Abe, and M. Kawamata, "A new variable step size LMS algorithm-based method for improved online secondary path modeling in active noise control systems," *IEEE Transactions on Audio, Speech, and Language Processing,* vol. 14, no. 2, pp. 720-726, 2006.

[6]   A. Carini and S. Malatini, "Optimal variable step-size NLMS algorithms with auxiliary noise power scheduling for feedforward active noise control," *IEEE Transactions on Audio, Speech, and Language Processing,* vol. 16, no. 8, pp. 1383-1395, 2008.

[7]   P. A. C. Lopes and J. A. Gerald, "Auxiliary Noise Power Scheduling Algorithm for Active Noise Control with Online Secondary Path Modeling and Sudden Changes," *IEEE Signal Process. Lett.,* vol. 22, no. 10, pp. 1590-1594, 2015.

[8]   T. Yang, L. Zhu, X. Li, and L. Pang, "An online secondary path modeling method with regularized step size and self-tuning power scheduling," *The Journal of the Acoustical Society of America,* vol. 143, no. 2, pp. 1076-1084, 2018.

[9]   S. M. Kuo and D. R. Morgan, "Active noise control: a tutorial review," *Proceedings of the IEEE,* vol. 87, no. 6, pp. 943-973, 1999.

[10]   T. Zhao, J. Liang, L. Zou, and L. Zhang, "A New FXLMS Algorithm With Offline and Online Secondary-Path Modeling Scheme for Active Noise Control of Power Transformers," *IEEE Transactions on Industrial Electronics,* vol. 64, no. 8, pp. 6432-6442, 2017.

[11]   D. Zhou and V. DeBrunner, "A new active noise control algorithm that requires no secondary path identification based on the SPR property," *IEEE Transactions on Signal Processing,* vol. 55, no. 5, pp. 1719-1729, 2007.

[12]   M. Wu, G. Chen, and X. Qiu, "An improved active noise control algorithm without secondary path identification based on the frequency-domain subband architecture," *IEEE Transactions on Audio, Speech, and Language Processing,* vol. 16, no. 8, pp. 1409-1419, 2008.

[13]   M. Gao, J. Lu, and X. Qiu, "A simplified subband ANC algorithm without secondary path modeling," *IEEE/ACM Transactions on Audio, Speech, and Language Processing,* vol. 24, no. 7, pp. 1164-1174, 2016.

[14]   M. Rotaru, F. Albu, and H. Coanda, "A variable step size modified decorrelated NLMS algorithm for adaptive feedback cancellation in hearing aids," in *2012 10th International Symposium on Electronics and Telecommunications*, 2012, pp. 263-266: IEEE.

[15]   S. Zhang, J. Zhang, and H. Han, "Robust Variable Step-Size Decorrelation Normalized Least-Mean-Square Algorithm and its Application to Acoustic Echo Cancellation," *IEEE/ACM Trans. Audio, Speech & Language Processing,* vol. 24, no. 12, pp. 2368-2376, 2016.

[16]   S. Zhang, H. C. So, W. Mi, and H. Han, "A Family of Adaptive Decorrelation NLMS Algorithms and Its Diffusion Version Over Adaptive Networks," *IEEE Transactions on Circuits and Systems I: Regular Papers,* vol. 65, no. 2, pp. 638-649, 2018.

[17]   S. M. Kuo and D. Morgan, *Active noise control systems: algorithms and DSP implementations*. John Wiley & Sons, Inc., 1995.

[18]   S. M. Kuo and D. R. Morgan, "Active noise control: a tutorial review," *Proceedings of the IEEE,* vol. 87, no. 6, pp. 943-973, 1999.